PROCEEDINGS, 44th Workshop on Geothermal Reservoir Engineering
Stanford University, Stanford, California, February 11-13, 2019
SGP-TR-214

Microseismic Signatures of Hydraulic Fracturing: A Preliminary Interpretation of Intermediate-Scale Data from the EGS Collab Experiment 1

Pengcheng Fu[1], Martin Schoenball[2], Joseph Morris[1], Jonathan Ajo-Franklin[2], Hunter Knox[3], Timothy Kneafsey[2], Jeffrey Burghardt[4], Mark White[4], and EGS Collab Team[5]

[1] Atmospheric, Earth, and Energy Division, Lawrence Livermore National Laboratory, Livermore, CA 94526

[2] Lawrence Berkeley National Laboratory, Berkeley, CA 94720

[3] Sandia National Laboratories, Albuquerque, NM, 87185

[4] Pacific Northwest National Laboratory, Richland, WA 99352

Email: fu4@llnl.gov

Keywords: EGS, Collab, hydraulic fracturing, microseismic

ABSTRACT

Microseismic monitoring is widely used to map the development of hydraulic fractures during stimulation of enhanced geothermal, as well as unconventional oil and gas reservoirs. While a prevalent practice is to infer the hydraulic fracture locations and extents based on the locations and shapes of microseismic "clouds", the occurrences of microseismic events are neither sufficient nor necessary conditions for the presence of a hydraulic fracture at the mapped locations. Definitively establishing the connection between microseismic events and hydraulic fractures is of a great importance. The EGS Collab project offers a unique opportunity to address this problem by enabling microseismic monitoring a short distance (tens of meters) from the events and providing multiple types of measurements and observations to corroborate the inferred fracture locations and extents. This work performs a detailed interpretation of the microseismic survey data for the hydraulic stimulation experiments conducted in May 2018. We compare the microseismic event locations to other indications of fracture development to discern the location of the hydraulic fracture with a high certainty. The results suggest that the resolved events were mostly associated with tensile fracturing events. They also suggest that a wide, permeable natural fracture referred to as the OT-P Connector deterred the propagation of the hydraulic fracture upon intersection, and that the hydraulic fracture bifurcated into two smaller planar features after crossing the OT-P Connector. There is no definitive evidence to support microseismic events generated by shearing of natural fractures.

INTRODUCTION

The EGS (enhanced geothermal system) Collab project, sponsored by the United States Department of Energy (DOE), Geothermal Technologies Office (GTO), focuses on intermediate-scale (~10-20 m) EGS reservoir creation processes and related model validation in crystalline rock. The first phase (referred to as "Collab Experiment 1" or "Experiment 1") of the project is underway at the West Access Drift of the Sanford Underground Research Facility (SURF) in South Dakota at 4850 ft (1478 m) below ground. This phase aims to create an EGS test bed through hydraulic fracturing, although it is understood that hydro-shearing and other forms of perturbation to the natural fractures could also take place during the stimulations.

The test bed of Experiment 1 is highly instrumented along six observations wells. A full suite of observations and measurements, including microseismicity, continuous active-source seismic monitoring (CASSM), step-rate injection method for fracture in-situ properties (SIMFIP), fiber-based distributed temperature sensing (DTS), electrical resistivity tomography (ERT), etc., during the stimulation and circulation tests were acquired. Knox et al., (2017) and Morris et al., (2018) provided comprehensive overviews of the design and instrumentation of the test bed. Kneafsey et al. (2019) provides the most current update of the status and achievements of the EGS Collab effort. This paper is primarily concerned with inferring the hydraulic fracture propagation trajectory and pattern from the microseismic events and connecting microseismicities to direct observations of the manifestations of the hydraulic fracture(s). Between May and

[5]J. Ajo-Franklin, S.J. Bauer, T. Baumgartner, K. Beckers, D. Blankenship, A. Bonneville, L. Boyd, S. Brown, S.T. Brown, J.A. Burghardt, T. Chen, Y. Chen, K. Condon, P.J. Cook, D. Crandall, P.F. Dobson, T. Doe, C.A. Doughty, D. Elsworth, J. Feldman, A. Foris, L.P. Frash, Z. Frone, P. Fu, K. Gao, A. Ghassemi, H. Gudmundsdottir, Y. Guglielmi, G. Guthrie, B. Haimson, A. Hawkins, J. Heise, M. Horn, R.N. Horne, J. Horner, M. Hu, H. Huang, L. Huang, K.J. Im, M. Ingraham, R.S. Jayne, T.C. Johnson, B. Johnston, S. Karra, K. Kim, D.K. King, T. Kneafsey, H. Knox, J. Knox, D. Kumar, K. Kutun, M. Lee, K. Li, R. Lopez, M. Maceira, P. Mackey, N. Makedonska, C.J. Marone, E. Mattson, M.W. McClure, J. McLennan, T. McLing, C. Medler, R.J. Mellors, E. Metcalfe, J. Miskimins, J. Moore, J.P. Morris, S. Nakagawa, G. Neupane, G. Newman, A. Nieto, C.M. Oldenburg, W. Pan, T. Paronish, R. Pawar, P. Petrov, B. Pietzyk, R. Podgorney, Y. Polsky, J. Popejoy S. Porse, B.Q. Roberts, M. Robertson, W. Roggenthen, J. Rutqvist, D. Rynders, H. Santos-Villalobos, M. Schoenball, P. Schwering, V. Sesetty, C.S. Sherman, A. Singh, M.M. Smith, H. Sone, F.A. Soom, C.E. Strickland, J. Su, D. Templeton, J.N. Thomle, C. Ulrich, N. Uzunlar, A. Vachaparampil, C.A. Valladao, W. Vandermeer, G. Vandine, D. Vardiman, V.R. Vermeul, J.L. Wagoner, H.F. Wang, J. Weers, J. White, M.D. White, P. Winterfeld, T. Wood, S. Workman, H. Wu, Y.S. Wu, Y. Wu, E.C. Yildirim, Y. Zhang, Y.Q. Zhang, J. Zhou, Q. Zhou, M.D. Zoback

December, 2018, hydraulic stimulations were performed on three pre-cut notches in stimulation well E1-I. We focus on observations from the multiple "episodes" of stimulation on the 164 ft (50 m) deep (MD, measured depth) notch in May and June 2018.

2. THE NATURAL FRACTURE SYSTEM

The host rock of the Experiment 1 test bed has a relatively extensive natural fracture system. Based on wellbore image logs and the continuous cores retrieved from the eight wells, 206 intersections between wellbores and natural fractures were identified and logged. Note that a fracture could intersect multiple wells and be logged multiple times. Broadly speaking, the natural fractures can be divided into three categories: 1. Naturally "flowing fractures", from or into which water can flow freely at pressure close to the atmospheric pressure; 2. visually "open fractures", with partially open aperture but no significant hydraulic conductivity; and 3. "sealed fractures" without apparent opening or hydraulic conductivity and sealed by mostly quartz. There are 5, 71, and 130 traces logged in these three categories, respectively. Figure 1 shows lower hemisphere stereographic projections of the natural fracture planes. Although the fractures have a wide range of orientations, the majority of natural fractures, particularly the flowing and open fractures, have NE-SW striking and steep dipping, forming a coherent natural fracture family/set. Particularly, four of the five flowing fractures belong to this family.

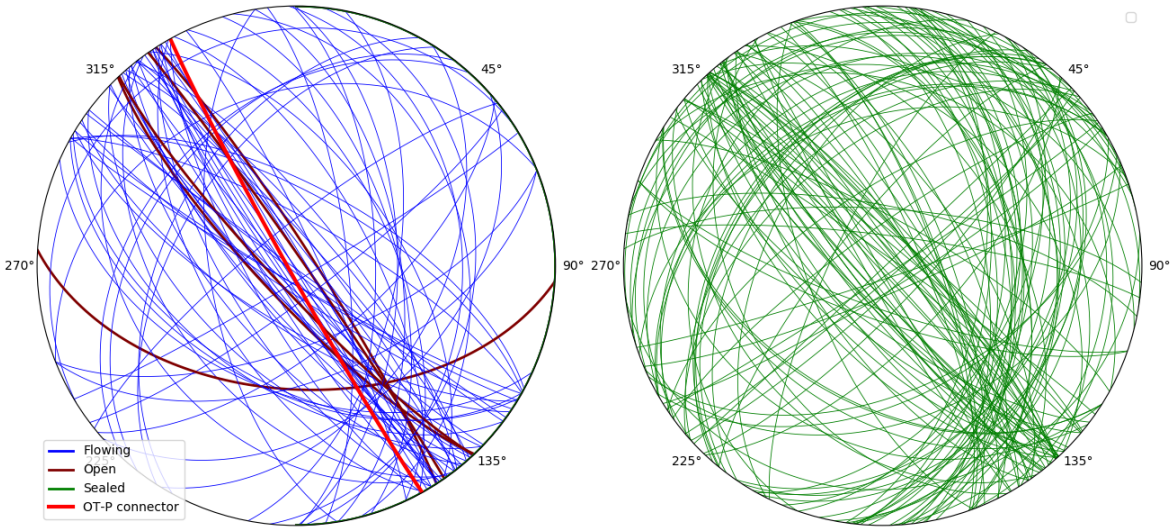

Figure 1: Stereonet projections of the flowing, open, and sealed natural fractures logged at the Experiment 1 test bed.

An important feature of the natural fracture system is that three flowing fracture traces and two open fracture traces in five different wells seem to conform to the same planar structure. The best-fit plane has a strike angle of 150.9° and a dipping angle of 87.5°. It is highly likely that these five traces belong to the same open natural fracture as illustrated in Figure 2 (a) and (b). This natural fracture is referred to as the "OT-P Connector" because fluid injected into the trace in E1-OT under low pressure flows out of the tracer in E1-P and vice versa. The cores retrieved from the corresponding depths in the five wells show that the OT-P Connector is filled with quartz of various thickness and has a partially open aperture of up to several millimeters. The OT-P Connector is approximately 10 m to the west of the stimulation notch. Hydraulic fracturing simulations performed in support of the test bed design [Fu et al., 2018] indicated a hydraulic fracture initiating from well E1-I would have a strong tendency to propagate toward the drift (mostly eastward). As the OT-P connector intersects the estimated fracture trajectory, such a wide, high-conductivity fracture is expected to significantly influence the behavior of the hydraulic fracture.

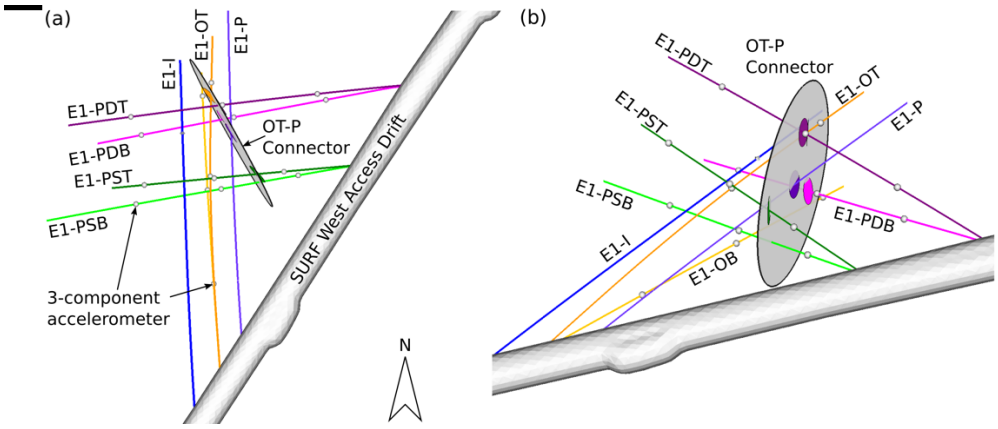

Figure 2: The spatial relationship between the drift, the eight wells, and the OT-P Connector.

3. HYDRAULIC STIMULATIONS

Microseismic activities from five stimulation "episodes" are considered in the current study. Three stimulation episodes took place on May 22 to May 24, one on each day, while two stimulations took place on May 25. These episodes are referred to as Stimulations 522, 523, 524, 525A, and 525B, respectively. Each episode was performed for specific objectives, but the plan was often adjusted in real-time based on the responses of the test bed observed in the field and the availability of equipment and resources. Stimulation 522 initiated the fracture and propagated the fracture to a calculated nominal radius of 1.5 m. Stimulation 523 further propagated the fracture to a nominal radius of 5 m. The objective of stimulation 524 was to further propagate the fracture to connect to well E1-P. Significant flow was observed in well E1-OT and well E1-P, respectively, after the injection was increased to 2.6 L/min and higher. Injection rates up to 5 L/min were used. Stimulation 525A largely repeated Stimulation 524 to make SIMFIP measurements in E1-I and E1-P. For stimulation 525B, a sewer camera was used to survey well E1-P during the injection to enable visual observations of the intersection(s) of the fracture(s) with this well. The stimulation parameters are summarized in Table 1, and the injection histories are shown in a continuous plot in Figure 3.

The sensor deployment and the data recording system for microseismic surveys are described in Schoenball [2019]. The automatically identified event trigger counts and the distances of the located microseismic events to the stimulation notch are plotted in Figure 3 along with the injection history.

Table 1 Summary of the stimulation activities concerned in the current work

Label	Date, in 2018	Duration (min) at rate > 0.05 L/min	Max. flow rate (L/min)	Total Inj. Vol. (L)
522	May 22	10.5	0.2	2.1
523	May 23	65.2	0.4	23.3
524	May 24	31.7	5.0	79.6
525A	May 25	31.5	4.6	77.8
525B	May 25	32	4.6	119.3

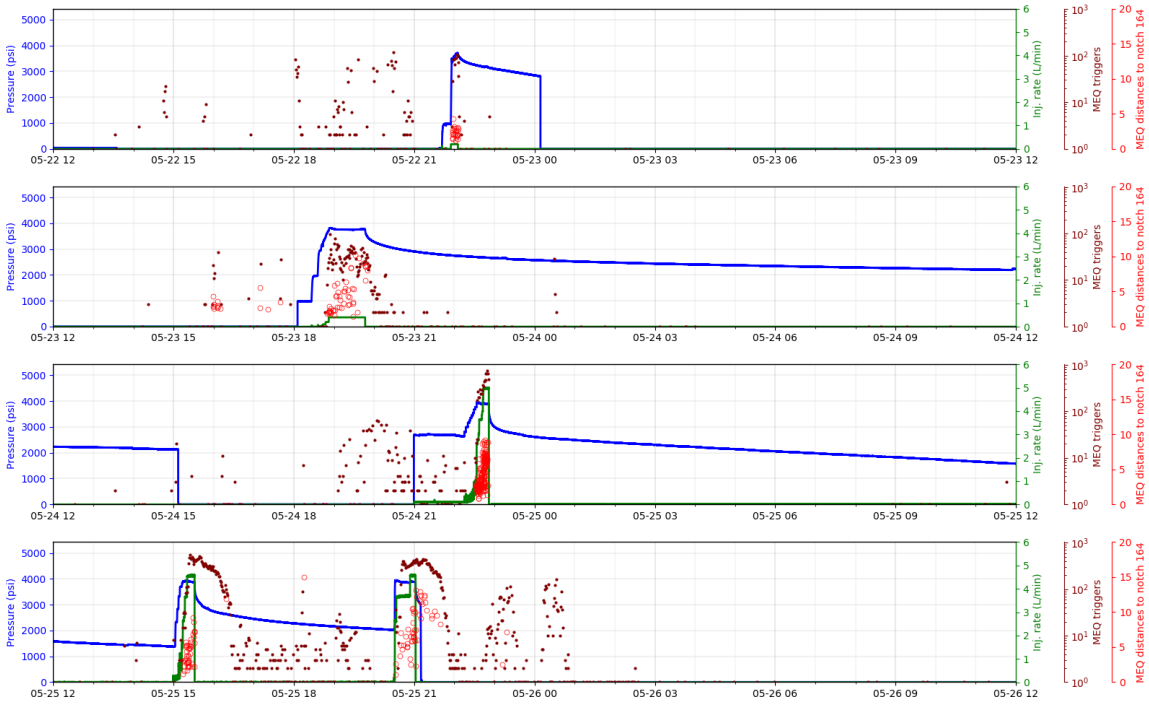

Figure 3: Injection activities in the five stimulation episodes visualized in a continuous fashion. The brown dots are the automatic event triggers per minutes recorded. Event triggers and microseismic events outside the stimulation windows were caused by activities in other wells or in the drift.

4. DIRECT OBSERVATIONS OF HYDRAULIC FRACTURE'S MANIFESTATIONS

4.1 Temperature anomalies in well E1-OT

A manifestation of the hydraulic fracture(s) was the observation of temperature anomalies in the form of sudden, mild temperature increase (< 2.0°C) at approximately 45 m deep in well E1-OT measured by DTS. Such an anomaly first appears at 19:30 UTC (Coordinated Universal Time) on May 23, in the middle of stimulation 523. A stronger DTS signal was observed at the same location at 22:40 UTC on May 24, during stimulation 534, a few minutes before outflow water was observed at the wellhead of E1-OT. Similar temperature anomalies were observed in the subsequent stimulations from E1-I: 525A and 525B. As shown in Figure 3, temperature anomalies appeared in two locations close to each other near 45 m depth in E1-OT. An inspection of the wellbore logs and core photos did not find any natural fractures in these locations, suggesting these temperature anomalies are likely the result of hydraulic fracture's intersections with the well.

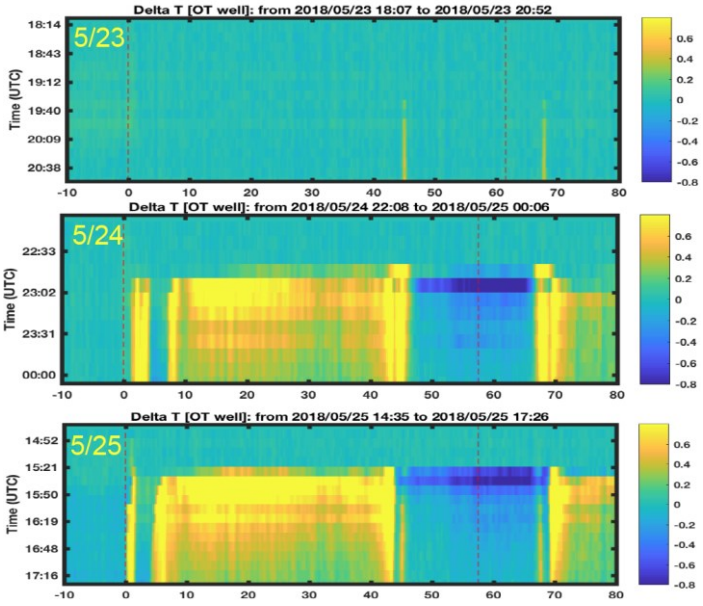

Figure 4: Temperature perturbations along well E1-OT caused by hydraulic stimulation on three separate days. The temperature difference (Delta T as noted in the figure) uses long-term average temperature as the baseline. Note that the depth is nominal and could be subject to further corrections. The temperature profile is expected to be symmetric against the well bottom depth because the same fiber loops back to the well collar.

4.2 Visible fracture intersections

During Stimulation 525B, a visual survey of well E1-P was performed using a sewer camera system. A thin stream of water was first observed approximately 15 minutes after the stimulation had started, and the "jetting" of water into the wellbore became more substantial thereafter in two clusters, at approximately 127 ft deep and 129 ft deep, respectively. Two snapshots of the jetting pattern are shown in Figure 5. The locations of the jetting spots have been carefully mapped on the well's televiewer log. The mapping results indicate that two or three hydraulic fracture planes intersected well E1-P. This is a particularly interesting observation considering the two closely spaced temperature anomalies in well E1-OT. We could infer that two closely spaced hydraulic fractures have been initiated and have propagated in a largely parallel fashion, which echoes observations of close fracture patterns in drill-back cores at major field experiments involving hydraulic fracturing (Raterman et al. 2017; Gale et al., 2018; Warpinski et al., 1993) . The mapping results also suggest that local fracture trajectories seem to have been influenced by the rock fabric (foliation planes and the folding of the foliation planes) while unaffected by the sealed natural fractures even when the hydraulic fractures intersect the natural fractures.

Connecting (1) the injection notch, at 164 ft (50m) MD in well E1-I, (2) the temperature anomaly in E1-OT at a nominal measured depth of 45 m or 148 ft, and (3) the mid-depth (128 ft or 39 m MD) of the two jetting clusters in E1-P yields a plane with a strike angle of 81° and dip angle of 74°. Note that this is only a 5° difference in strike and 4° difference in dip from the expected hydraulic fracture plane in the original test bed design. Since the test bed design was based on prior hydraulic fracturing results in a nearby vertical well stimulated in the kISMET (Oldenburg et al., 2016) experiment, this inferred hydraulic fracture plane is consistent with hydraulic fracture orientations in the same rock formation a short distance away and implies that the stress orientations at the two locations are similar.

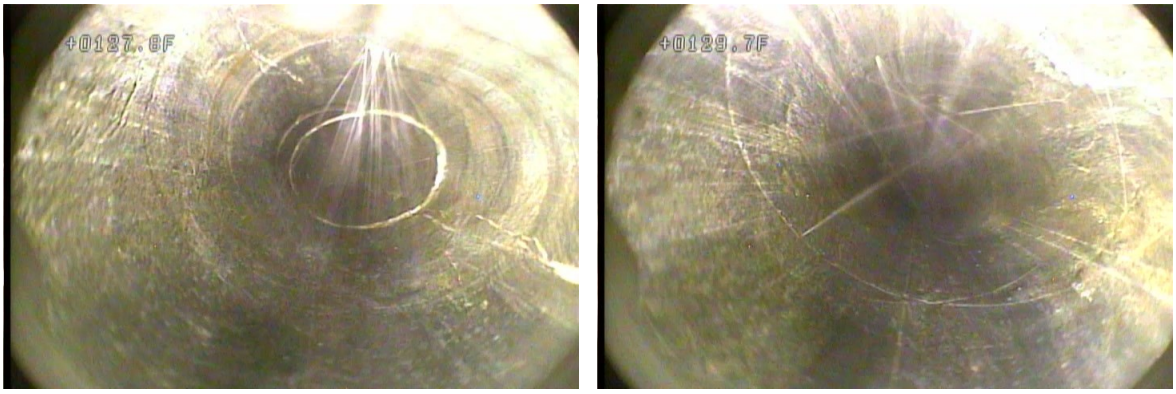

Figure 5: Two snapshots of the sewer camera footage showing water jetting at approximately 127 ft (left) and 129 ft (right) deep in well E1-P. The depth measurements on images are nominal.

5. ANALYSIS OF THE MICROSEISMIC EVENTS

5.1 The overall pattern of microseismic cloud

The deployment of the sensor array, the data acquisition program, as well as the data processing methodology is described in Schoenball et al. (2019) and not repeated here. Approximately 400 microseismic events were located in the concerned time window between May 22 and May 25, as displayed in Figure 6 in three view angles. The following patterns can be observed.

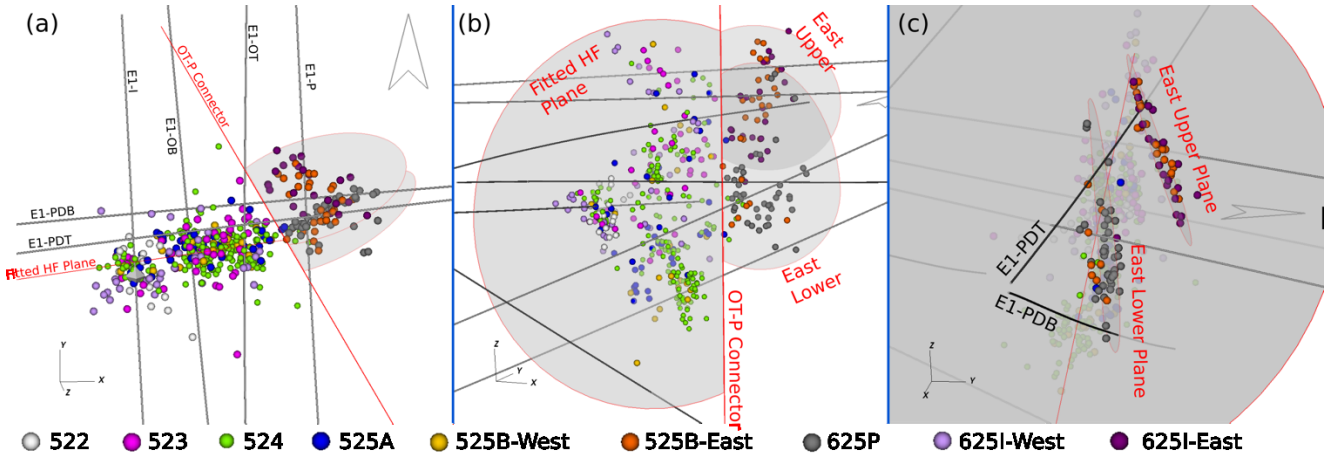

Figure 6: Spatial distribution of the microseismic events in the concerned period. Events from a later stimulation on June 25 are also shown for reference. The events are colored based on the dates of stimulation and whether the events were to the west or east of OT-B connector. (a) A top view along the intersection line between the fitted hydraulic fracture plane and the OT-P connector plane; (b) a side view along the OT-P connector plane; and (c) a side view from the east of OT-P connector. Note the triad indicates the directions of east (x), north (y), and up (z).

- The OTP Connector behaved as an apparent barrier to fracture growth, or more strictly speaking, to the propagation of the fracture's microseismic footprint. In both Stimulation 524 and Stimulation 525A, microseismic events appeared near the OT-P Connector well before the terminations of the stimulations but continued injection did not produce microseismic events to the east of the OT-P Connector. However, the OT-P Connector deterred but did not completely prevent the eastward propagation of the microseismic cloud during subsequent injections. Stimulation 525B, which involved a larger injection volume than Stimulations 524 and 525B, produced substantial microseismic events to the east of the OT-P Connector near the end of injection.
- The microseismic cloud west of the OT-P Connector combining all the five stimulation episodes between May 22 and May 25 seems to conform to a planar, largely vertical structure. A linear regression shows that the best-fit plane has a strike angle of 83° and a dip angle of 74°, strikingly similar to a plane that spans the fracture's directly-observed manifestations (81° and 74°, respectively). The standard deviation of the events' distances to the best-fitted plane is 0.7 m, in the same order of magnitude as the estimated locating error. Regressions on the events from individual stimulation episodes show that the clouds from 523, 524, 525A, and 525B, conform to the same plane with a relatively small difference between them.

- This fracture plane to the west of OT-P Connector did not continuously extend to the east side of the OT-P Connector. Instead, two distinct, relatively small planar features developed in a somewhat parallel fashion. The corresponding events from separate stimulation episodes collocated along the two planes in a highly coherent way, implying high certainty in the inferred locations and orientations of these two features.
- On the inferred fracture plane to the west of OT-P Connector, seismic event clusters from different stimulation episodes seem to rarely overlap, suggesting that different areas on the plane were seismically "activated" by different stimulations. An area that had been activated by a prior stimulation tended to be seismically "silent" in subsequent stimulations. This suggests the microseismic events are associated with the creation of new fracture surface rather than the shearing of nature fractures due to pressure diffusion.

5.2 The relationship among various inferred plane features

The stereonet projections of several planar features concerned in the current study are show in Figure 7. The most striking observation is the high consistency between the orientations, determined with independent methods, of the main hydraulic fracture plane to the west of OT-P Connector. These methods include:

- The average hydraulic fracture orientation in the nearby kISMET experiment.
- The triangle spanning the directly observed manifestations of the hydraulic fracture(s) at three wells.
- Linear regressions on the microseismic events, including regressions on events from individual stimulations.

Therefore, the main hydraulic fracture plane has been determined with relatively high certainty. A comparison between Figure 7 and Figure 1 shows that there is not a natural fracture set with an overall orientation consistent with the orientations of the two microseismic planar features to the east of OT-P Connector. This suggests that these two features are likely opening-mode fractures as well.

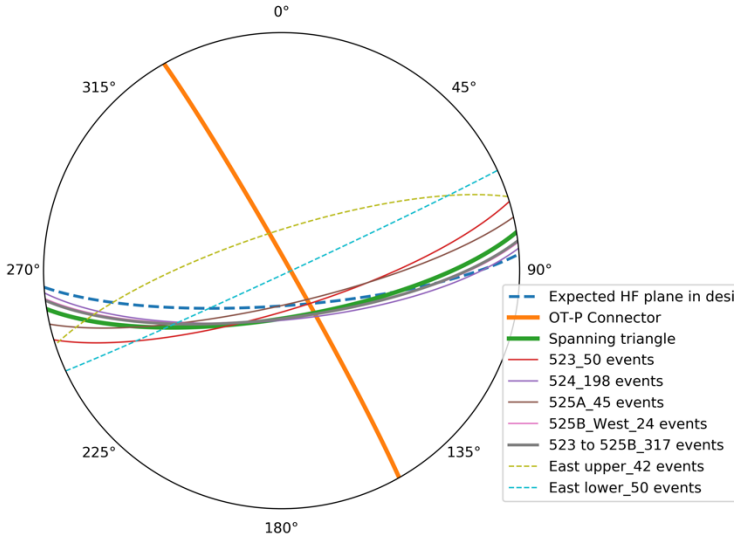

Figure 7: Stereonet projections of nine plane features concerned in this study. If the plane is based on regression on microseismic events, the number of events involved is noted on the legend.

6. CONCLUSIONS

This work attempts to provide a preliminary interpretation of the microseismic survey results from EGS Collab Experiment 1's first set of hydraulic stimulation experiments. As data processing continues and more thorough and detailed data analyses are underway, we present the following preliminary conclusions:

The microseismic events in the current catalogue show high consistency with other observations and measurements. For example, the eastward propagation of the seismic cloud was deterred at a known feature, namely the OT-P Connector; the time of temperature anomalies in E1-OT coincided with when the microseismic cloud reached that well; and so on. This consistency builds confidence in the quality of the measurements and data processing.

The main hydraulic fractures/features stimulated between May 22 and May 25 from the 164 ft (50 m) notch in E1-I have been discerned. One relatively large hydraulic fracture (or a pair of fractures) was created and was partially arrested by the OT-P Connector. The orientation of this main fracture was determined with three independent methods, resulting in a small variation margin. This fracture seemed to have bifurcated into two smaller fractures to the east of OT-P Connector. Note that although other planar features oblique to the main hydraulic fracture direction could be identified in the microseismic cloud (Schoenball et al., 2019) to the west of the OT-P

Connector purely from the form of the cloud, their effects on the test bed cannot be assessed unless definitive evidence emerges to corroborate their presence and provide more information regarding their nature.

Both the main fractures and the two bifurcated wings are likely opening-mode hydraulic fractures, because (1) the rock formation does not have a natural fracture system in the corresponding orientations, and (2) the microseismic clusters generated by different episodes of stimulation do not significantly overlap.

The observations described in the current work reveal two distinct roles of natural fractures regarding their interactions with hydraulic fractures. First, open, hydraulically conductive natural fractures could deter the propagation of hydraulic fractures. However, the major nature fracture encountered in this experiment, the OT-P Connector, did not completely arrest the hydraulic fracture(s), despite its very large aperture and the relatively low volumetric flux of the stimulations. Instead, the hydraulic fracture bifurcated when crossing this natural fracture. The distinct orientations of the fractures at the two sides of the OT-P Connector suggest that this natural fracture could be the boundary of different *in situ* stress regimes. Second, closed/sealed natural fractures did not seem to have any significant effect on the propagation of the hydraulic fracture. There is no indication of slipping of these natural fractures to generate microseismic events.

We also saw evidence in two independent observations, namely temperature anomalies in one well and visible water streams in another, to support the possibility of closely spaced hydraulic fractures propagating in a largely parallel fashion. This could provide definitive evidence to corroborate similar observations from drill-back experiments in recent large-scale hydraulic fracturing field experiments.

ACKNOWLEDGMENTS:

This manuscript has been authored by Lawrence Livermore National Security, LLC under Contract No. DE-AC52-07NA27344 with the US. Department of Energy. This research was also supported by the U.S. Department of Energy, Geothermal Technologies Office (GTO). The United States Government retains, and the publisher, by accepting the article for publication, acknowledges that the United States Government retains a non-exclusive, paid-up, irrevocable, world-wide license to publish or reproduce the published form of this manuscript, or allow others to do so, for United States Government purposes. We thank the drillers of Agapito Associates, Inc., for their skill and dedicated efforts to create our test bed boreholes. The research supporting this work took place in whole or in part at the Sanford Underground Research Facility in Lead, South Dakota. The assistance of the Sanford Underground Research Facility and its personnel in providing physical access and general logistical and technical support is gratefully acknowledged.

REFERENCES

Fu, P., M. White, J. Morris, T. Kneafsey, and E.C. Team (2018), Predicting Hydraulic Fracture Trajectory Under the Influence of a Mine Drift in EGS Collab Experiment I, in *PROCEEDINGS, 44th Workshop on Geothermal Reservoir Engineering*, Stanford University, Stanford, CA (2018).

Gale, J.F.W., Elliott, S.J., and Laubach, S.E.: Hydraulic Fractures in Core From Stimulated Reservoirs: Core Fracture Description of HFTS Slant Core, Midland Basin, West Texas (2018), doi:10.15530/urtec-2018-2902624.

Kneafsey, T.J., Blankenship, D., Hunter K.A., Johnson T.C., Ajo-Franklin J.B., Schwering, P.C., Dobson P.F., Morris, J.P., White, M.D., Fu, P., Podgorney, R., Roggenthen, W., Doe, T., Mattson, E., Ghassemi, A., Valladao, C. and the EGS Collab team: EGS Collab Project: Status and Progress, *Proceedings,* 44th Workshop on Geothermal Reservoir Engineering, Stanford University, Stanford, CA (2019)

Knox, H., Fu, P., Morris, J.P., Guglielmi, Y., Vermeul, V., Ajo-Franklin, J, Strickland, C., Johnson, T., Cook, P., Herrick, C., Lee, M. and the EGS Collab team (2017), Fracture and Flow Designs for the Collab/Sigma-V Project in GRC Transactions, Vol. 41, 2017.

Morris, J.P., P. Dobson, H. Knox, J. Ajo-Franklin, M.D. White, P. Fu, J. Burghardt, T.J. Kneafsey, D. Blankenship, and the EGS Collab team: Experimental Design for Hydrofracturing and Fluid Flow at the DOE Collab Testbed in *PROCEEDINGS, 44th Workshop on Geothermal Reservoir Engineering*, edited, Stanford University, Stanford, California (2018).

Oldenburg, C.M., P.F. Dobson, Y. Wu, P.J. Cook, T.J. Kneafsey, S. Nakagawa, C. Ulrich, D.L. Siler, Y. Guglielmi, J. Ajo-Franklin, J. Rutqvist, T.M. Daley, J.T. Birkholzer, H. Wang, N.E. Lord, B.C. Haimson, H. Sone, P. Vigilante, W.M. Roggenthen, T.W. Doe, M.Y. Lee, M. Ingraham, H. Huang, E.D. Mattson, J. Zhou, T.J. Johnson, M.D. Zoback, J.P. Morris, J.A. White, P.A. Johnson, D. DD. Coblentz, and J. Heise.: *Intermediate-Scale Hydraulic Fracturing in a Deep Mine, kISMET Project Summary 2016*, LBNL-1006444, Lawrence Berkeley National Laboratory, Berkeley, CA (2016). DOI: 10.2172/1338937.

Raterman, K.T, Farrell, H.E., Mora, O.S., et al.: Sampling a Stimulated Rock Volume: An Eagle Ford Example" (2017), doi:10.15530/urtec-20172670034.

Schoenball, M., Ajo-Franklin, J., Blankenship, D., Cook, P., Dobson, P., Guglielmi, Y., Fu, P., Kneafsey, T., Knox, H., Petrov, P., Robertson, M., Schwering, P., Templeton, D., Ulrich, C., Wood, T., and the EGS Collab Team: Microseismic Monitoring of Meso-Scale Stimulations for the DOE EGS Collab Project at the Sanford Underground Research Facility, in *PROCEEDINGS*, 44th Workshop on Geothermal Reservoir Engineering, edited, Stanford University, Stanford, California (2019),.

Warpinski, N.R., Lorenz, J.C. Branagan, P.T., Myal, F.R., Gall, B.L., Examination of a Cored Hydraulic Fracture in a Deep Gas Well, SPE-22876-PA, (1993)